Articles

Metallocene-Mediated Asymmetric Coordination Polymerization of Polar Vinyl Monomers to Optically Active, Stereoregular Polymers

Garret M. Miyake and Eugene Y.-X. Chen*

Department of Chemistry, Colorado State University, Fort Collins, Colorado 80523-1872

Received January 10, 2008; In Final Form February 18, 2008;
Revised Manuscript Received February 17, 2008

ABSTRACT: Asymmetric coordination polymerization of 13 acrylamide and methacrylate monomers of four different classes has been investigated using chiral *ansa*-zirconocenium ester enolate catalyst (*S,S*)-(EBI)Zr^+(THF)[OC(O*i*Pr)═CMe_2][$MeB(C_6F_5)_3$]$^-$ [(*S,S*)-**1**), EBI = $C_2H_4(\eta^5\text{-Ind})_2$] and its enantiomer (*R,R*)-**1**. This polymerization system is built upon four advanced features of polymerization including living, stereospecific, coordination, and asymmetric core elements, thus efficiently converting prochiral *N,N*-diaryl acrylamides at ambient temperature to optically active, stereoregular polymers with solution-stable, single-handed helical secondary structures. Kinetic studies show that the polymerization of *N,N*-diaryl acrylamides by **1** proceeds via a monometallic, coordination-conjugate addition mechanism. Investigation into polymer chain-length effects on optical activity of the chiral polymers reveals two opposite trends, depending on the polymer secondary structure (i.e., helical vs random coil conformation). Examination of the polymerization scope shows that the formation of optically active poly(acrylamide)s due to solution-stable helical conformations with an excess of one-handed helicity is dictated by the sterics and rigidity of the monomer repeat units; while diaryl acrylamides can readily achieve such conformations, unsymmetrically substituted diaryl acrylamides give the chiral polymers with much higher optical activity than the symmetrically substituted ones. It is also possible for *N,N*-dialkyl acrylamides to lead to chiral helical polymers. Extensive asymmetric block copolymerization studies of MMA with acrylamides and other methacrylates have also been carried out, producing optically active, high-molecular-weight methacrylate-*b*-acrylamide stereoblock copolymers in which the acrylamide block can be either helical or nonhelical; in sharp contrast, all high-molecular-weight methacrylate-*b*-methacrylate di- or triblock copolymers produced by the enantiomeric catalysts **1** are optically inactive.

Introduction

Optically active chiral polymers are not only fundamentally interesting, due to the rich and complex architecture of macromolecular chirality as compared to that of small molecules, but also technologically important because their unique chiral arrays give rise to a number of potential, and in some cases commercially implemented, applications.[1] In the case of stereoregular vinyl polymers[2] with configurational main chain chirality derived from 1-substituted or nonsymmetric 1,2-disubstituted vinyl monomers (i.e., technologically most important polymers) without chiral side groups, such enantiomerically pure or enriched polymers cannot be optically active because the entire polymer chain (by the infinite chain model) contains a mirror plane (for isotactic polymers) or a glide mirror plane and translational mirror planes perpendicular to the chain axis (for syndiotactic polymers), and thus are achiral.[1] Low-molecular-weight (MW) isotactic oligomers of propylene,[3] 1-butene,[4] and other α-olefins[5] produced by optically active *ansa*-zirconocene catalysts showed measurable optical activity, but high-MW isotactic polypropylene (*it*-PP) produced by the similar enantiomeric chiral catalyst did not have a detectable optical activity in solution and in the melt.[6] As a polymer chain becomes long enough its chain-end groups impose negligible effects on the chiroptical properties of the polymer; thus, an enantiomerically pure or enriched polymer of low enough MW and containing nonequivalent chain-end groups can be optically active, as shown by the above oligomeric α-olefin examples. Wulff et al. determined at which degree of polymerization (P_n) the optical activity of enantiomerically pure or enriched isotactic poly(methyl methacrylate), P(MMA), in a random-coil conformation with different chain ends, is still observable ($[\alpha]^{20}_{546}$ = −3.0° to −0.5° for M_n = 3050−26 050) as a result of elimination of the mirror plane by the chain-end groups;[7] only at a very high P_n (>300) does the optical activity become negligible, and the polymer then becomes *cryptochiral*. On the other hand, Okuda and co-workers recently employed enantiomerically pure nonmetallocene titanium catalysts for the asymmetric polymerization of styrene and found that P_n at which optically active isotactic oligomeric styrenes ($[\alpha]^{23}_D$ = ± 5.9−1.5°) became cryptochiral with no measurable optical activity in solution is rather low (<45).[8] In short, it appears that polar functionalized vinyl polymers such as P(MMA) develop the cryptochiral phenomenon at a considerably higher degree of polymerization than that for nonpolar polyolefins.

Three major strategies that do not rely on chain-end groups or chiral auxiliaries to eliminate reflection elements of symmetry of stereoregular vinyl polymers have been developed for the synthesis of *high-MW, chiral polymers* derived from prochiral vinyl monomers. First, chiral template-mediated polymerization utilizes styrene derivatives carrying optically active, removable mannitol template groups at the 4-position to radically copo-

* To whom correspondence should be addressed. E-mail: eychen@lamar.colostate.edu.

10.1021/ma8000675 CCC: $40.75
Published on Web 04/30/2008

Chart 1. Synthesis of Right- And Left-Handed Rigid Helical Poly(*N*,*N*-diaryl acrylamide)s and Their Rigid Rod−Random Coil Block Copolymers With MMA

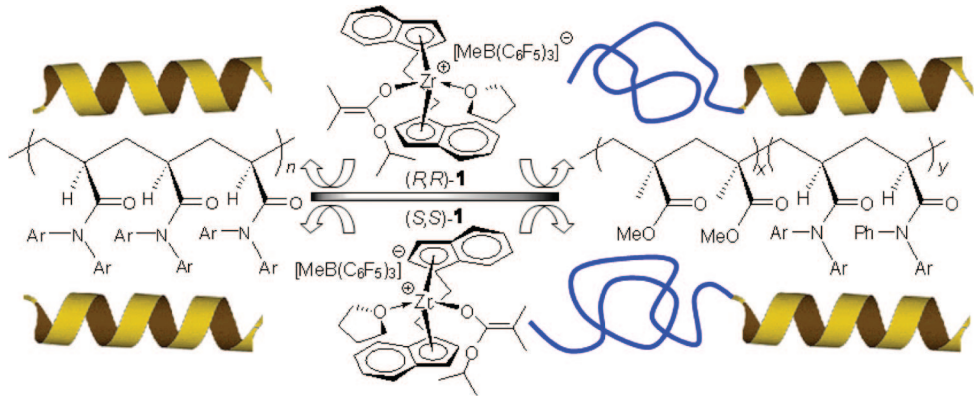

lymerize with styrene and subsequently convert the copolymer to an optically active polystyrene ($[\alpha]^{30}_{365} = -0.5$ to $-3.5°$).[9] The optical activity was attributed to the presence of chiral dyads (in this case, the dyad has an (*S,S*) configuration) separated by atactic sequences, and other optically active vinyl polymers and copolymers of complex configurational architectures can be prepared in a similar manner.[10] Second, asymmetric cyclopolymerization of 1,5-hexadiene with enantiomerically pure zirconocene[11] or Salan−zirconium[12] catalysts produces optically active poly(methylene-1,3-cyclopentane), the optical activity of which is due to the presence of predominantly trans isotactic structures devoid of mirror planes of symmetry.[11] Third, asymmetric anionic polymerization of functionalized vinyl monomers containing bulky side groups (e.g., triarylmethyl methacrylates[13] and *N*,*N*-diaryl acrylamides[14]) with chiral organolithium initiators affords optically active polymers with rigid one-handed, solution-stable helical conformations rendered by steric repulsion of the bulky side groups of the highly isotactic polymers accessible through the helix-sense-selective polymerization.[15] This strategy of using such bulky vinyl monomers has also been extended to asymmetric radical polymerization leading to optically active isotactic helical polymers.[16] Many stereoregular vinyl polymers can have a secondary structure of helical conformations in the solid state (e.g., *it*-PP); however, they adopt on-average random-coil conformations in solution due to the fast solution dynamics of the polymer chain with low helix inversion barriers. Thus, *it*-PP produced by an optically active zirconocene catalyst exhibits a large optical rotation in suspension, but the optical activity is lost when the polymer is completely dissolved or heated.[6] Likewise, the large optical activity of helical poly(trityl methacrylate) almost vanishes with only a very small residual rotation when the bulky trityl groups are replaced with the methyl groups to give random-coil cryptochiral P(MMA).[13] Although the optical activity is lost, the enantiomeric nature of the polymer is maintained; thus, treatment of enantiomeric *it*-P(MMA) with achiral syndiotactic P(MMA) forms a double-stranded helical stereocomplex,[17] a chiral superstructure.[18]

We have recently developed the *living, stereospecific, and coordination* polymerization of functionalized vinyl monomers such as methacrylates utilizing the highly active racemic (*R*,*R*)/(*S*,*S*) *ansa*-zirconocenium catalyst, *rac*-(EBI)Zr^+(THF)-[$OC(O^iPr)$=CMe_2][$MeB(C_6F_5)_3$]$^-$ [*rac*-**1**; EBI = $C_2H_4(\eta^5$-$Ind)_2$], under ambient conditions.[19] The polymers produced were highly isotactic (>95% *mm* for P(MMA); >99% *mm* for P(*n*-butyl methacrylate), P(BMA), and had narrow molecular weight distributions (MWD = $M_w/M_n = 1.03$). The polymerization of methacrylates by *rac*-**1** is enantiomorphic-site controlled, proceeding through a monometallic, intramolecular Michael addition mechanism via eight-membered-ring cyclic ester enolate resting intermediates.[20] The coordination polymerization of acrylamides such as *N*,*N*-dimethyl acrylamide (DMAA) by this highly active catalyst system also proceeds in a living, isospecific, site-controlled manner, producing high-MW poly(*N*,*N*-dimethyl acrylamide), P(DMAA), with a narrow MWD of $M_w/M_n = 1.07$, a quantitative isotacticity of *mm* > 99%, and a high melting transition temperature of T_m > 307 °C.[21] Most recently, we have built the fourth, *asymmetric* element into our polymerization system and successfully developed asymmetric coordination polymerization of *N*,*N*-diaryl acrylamides such as *N*,*N*-diphenyl acrylamide (DPAA) and *N*-phenyl-*N*-(4-tolyl)acrylamide (PTAA) using enantiomeric catalysts (*S*,*S*)-**1** and (*R*,*R*)-**1** to produce the corresponding optically active, one-handed helical poly(*N*,*N*-diaryl acrylamide)s, P(DPAA) and P(PTAA), as well as their rigid rodlike block copolymers with random-coil P(MMA) blocks (Chart 1).[22]

Among the three major strategies developed for the synthesis of chiral vinyl polymers overviewed above, the asymmetric anionic polymerization using chiral organolithium initiators, pioneered by Okamoto and co-workers,[13,14] also deals with functionalized vinyl monomers (which bear bulky side groups). However, such polymerization must be carried out at low temperatures (−78 °C or lower) to achieve an appreciable level of polymerization control, as well as the polymer isotacticity and optical activity. Furthermore, in the chiral-initiator-controlled polymerization the enchaining monomer experiences varied degrees of asymmetric induction as a function of the growing chain length, giving rise to a large disparity in stereoregularity and optical activity of the polymer; even in the chiral-ligand-controlled anionic polymerization, such disparity still exists.[14a] In comparison, the recently developed asymmetric coordination polymerization system[22] exhibits the following three advanced features: (a) the living/controlled polymerization can be achieved at ambient temperature, (b) it exhibits a high degree of control in polymerization stereospecificity, which is much less sensitive to polymerization temperature because of its site-control nature, and (c) the reaction proceeds in a manner such that each enchaining monomer must coordinate to the chiral catalyst center before enchainment and is regulated by the same degree of chiral induction of the same asymmetric catalyst center, thereby producing chiral polymers of uniform asymmetric induction.

In our continuing studies of the asymmetric coordination polymerization of polar vinyl monomers such as acrylamides and methacrylates using enantiomeric chiral *ansa*-zirconocenium catalysts (*S*,*S*)-**1** and (*R*,*R*)-**1** and following our initial communication,[22] the current contribution focuses on the mechanism and scope (Chart 2) of this polymerization system and presents a full account of our investigation into (a) characteristics and kinetics of the polymerization of diaryl acrylamides, (b) effects of the chain length of helical and nonhelical poly(acrylamide)s

Chart 2. List of Acrylamide and Methacrylate Monomers (Grouped into Four Classes) Investigated in the Current Asymmetric Coordination Polymerization Study

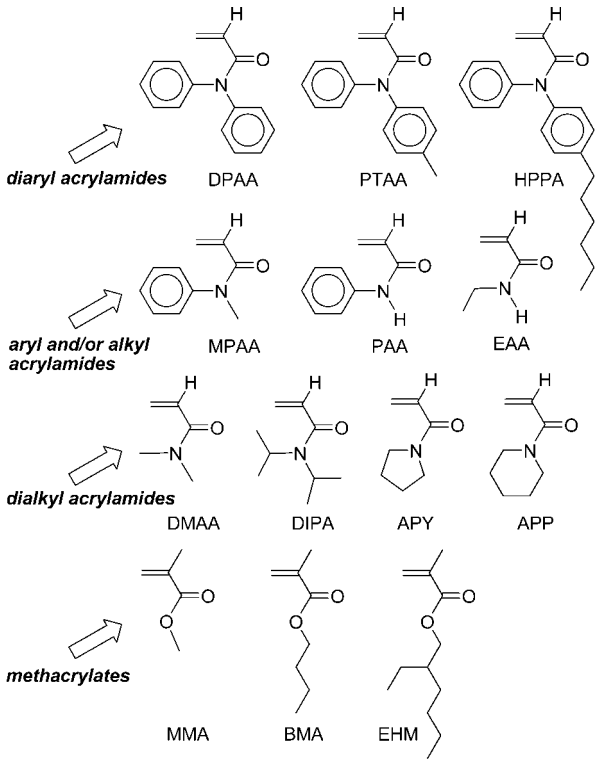

on optical activity, (c) the necessity of the *N*,*N*-diaryl side groups to render solution-stable helical conformations, (d) strategies to render solution solubility of rigid helical homopolymers by forming block copolymers with randomly coiled MMA blocks and by substitution in the aryl rings with a long-chain alkyl group, and (e) the ability of these enantiomeric catalysts to produce nonhelical, optically active block copolymers.

Experimental Section

Solvents and Methods. All syntheses and manipulations of air- and moisture-sensitive materials were carried out in flamed Schlenk-type glassware on a dual-manifold Schlenk line, a high-vacuum line, or in an argon- or nitrogen-filled glovebox. HPLC grade organic solvents were sparged extensively with nitrogen during filling of the solvent reservoir and then dried by passage through activated alumina (for THF, Et_2O, and CH_2Cl_2) followed by passage through Q-5-supported copper catalyst (for toluene and hexanes) stainless steel columns. Toluene-d_8 and benzene-d_6 were degassed, dried over sodium/potassium alloy, and filtered before use, whereas $CDCl_3$, CD_2Cl_2, and 1,2-$C_6H_4Cl_2$ were degassed and dried over activated Davison 4 Å molecular sieves. NMR spectra were recorded on either a Varian Inova 300 (FT 300 MHz, ^{1}H; 282 MHz, ^{19}F) or a Varian Inova 400 spectrometer. Chemical shifts for ^{1}H were referenced to internal solvent resonances and are reported as parts per million relative to tetramethylsilane, whereas ^{19}F NMR spectra were referenced to external $CFCl_3$.

Commercial Reagents. Diethylene glycol dimethyl ether, *n*-BuLi (1.6 M in hexanes), butylated hydroxytoluene (BHT-H, 2,6-di-*tert*-butyl-4-methylphenol), *p*-toluidine, indene, 1,2-dibromoethane, tetrachlorozirconium, triflic acid, lithium dimethylamide, diisopropylamine, piperidine, triethylamine, aniline, sodium azide, 1,1,3,3-tetramethyl guanidine, (2*S*,4*S*)-pentanediol (99% ee, $[\alpha]^{20}_D$ = +39.8, *c* = 10, $CHCl_3$), (2*R*,4*R*)-pentanediol (97% ee, $[\alpha]^{21}_D$ = −40.4, *c* = 10, $CHCl_3$), $(CF_3SO_2)_2O$, $PhBCl_2$, MeMgI (3.0 M in diethyl ether), 1,2-dibromobenzene, and CF_3COOH were purchased from Sigma-Aldrich. Diphenylamine, acryloyl chloride, copper(I) iodide, iodobenzene, *N*,*N*-dimethyl aniline, pyrrolidine, and 2,6-dimethylpyridine were purchased from Alfa Aesar. Trimethylaluminum (neat) and tri(*n*-octyl)aluminum (neat) were purchased from Strem Chemical Co., whereas isopropyl isobutyrate and *N*-methyl aniline were purchased from TCI America. The above commercial reagents were used as received, except for the reagents described below. Diethylene glycol dimethyl ether, indene, 1,2-dibromoethane, *N*,*N*-dimethyl aniline, acryloyl chloride, and iodobenzene were degassed using three freeze–pump–thaw cycles. *p*-Toluidine, $(CF_3SO_2)_2O$, and $PhBCl_2$ were vacuum-distilled. 2,6-Dimethylpyridine, isopropyl isobutyrate, aniline, diisopropylamine, piperidine, triethylamine, and pyrrolidine were degassed and dried over CaH_2 overnight, followed by vacuum distillation. BHT-H was recrystallized from hexanes prior to use. 1,4-Dioxane (Fisher Scientific) was degassed, dried over sodium/potassium alloy, and vacuum-distilled. Tris(pentafluorophenyl)borane $B(C_6F_5)_3$ was obtained as a research gift from Boulder Scientific Co. and further purified by recrystallization from hexanes at −30 °C.

Monomers (a Total of 13). Methyl methacrylate (MMA) and *n*-butyl methacrylate (BMA) were purchased from Sigma-Aldrich, while 2-ethylhexyl methacrylate (EHM) and *N*,*N*-dimethyl acrylamide (DMAA) were purchased from TCI America; the above four monomers were first degassed, dried over CaH_2 overnight and then vacuum transferred. Further purification of MMA involved titration with neat tri(*n*-octyl)aluminum to a yellow end point,[23] followed by distillation under reduced pressure. Literature procedures were used to prepare monomers *N*,*N*-diphenyl acrylamide (DPAA),[24] *N*-phenyl-*N*-(4-tolyl) acrylamide (PTAA),[14a] and *N*-(4-hexylphenyl)-*N*-phenyl acrylamide (HPPA).[14a] DPAA and PTAA were purified by three recrystalizations from a toluene/hexanes solvent mixture, whereas HPPA was purified by silica gel chromatography (eluent: hexane/diethyl ether = 3:1) and dried over CaH_2 overnight, followed by vacuum distillation. Other acrylamide monomers were prepared and purified in a similar manner. Specifically, *N*,*N*-diisopropyl acrylamide (DIPA), *N*-methyl-*N*-phenyl acrylamide (MPAA), *N*-phenyl acrylamide (PAA), acryloyl pyrrolidine (APY), and acryloyl piperidine (APP) were prepared by reacting 2 equiv of the appropriate amine with 1 equiv of acryloyl chloride in toluene at 0 °C and gradually warming the reaction mixtures to room temperature overnight with vigorous stirring. *N*-Ethyl acrylamide (EAA) was prepared by purging a solution of acryloyl chloride in toluene with ethylamine at 0 °C and then warming the reaction mixture to room temperature overnight with vigorous stirring. MPAA was purified by three recrystallizations from a toluene/hexanes solvent mixture, while DIPA, APY, APP, and EAA were purified by distillation and drying over CaH_2 overnight followed by additional vacuum distillation. PAA was purified by recrystallizations first from acetone and then from CH_2Cl_2. All purified monomers were stored in brown bottles kept inside a −30 °C glovebox freezer.

Noncommercial Reagents or Intermediates. The $(C_6F_5)_3B\cdot$THF adduct was prepared by addition of THF to a toluene solution of the borane followed by removal of the volatiles and drying in vacuo. Literature procedures were employed for the preparation of the following compounds and metallocene complexes: LiOC(O^{i}Pr)=CMe_2 [Li(IPIB)],[25] (EBI)H_2,[26] *rac*-(EBI)Zr$(NMe_2)_2$,[27] *rac*-(EBI)-$ZrMe_2$,[27] *rac*-(EBI)ZrMe(OTf),[19] *rac*-(EBI)ZrMe[OC(O^{i}Pr)=C-Me_2],[19] *rac*-(EBI)Zr$^+$(THF)[OC(O^{i}Pr)=CMe_2][MeB$(C_6F_5)_3$]$^-$(**1**),[19] (*S*,*S*)-(EBI)$ZrCl_2$,[28] and (*R*,*R*)-(EBI)$ZrCl_2$.[28]

Synthesis of Enantiomeric Catalysts 1. Scheme 1 outlines the entire 11-step synthesis of (*S*,*S*)-**1** starting from enantiopure 2,4-pentanediol to *S*,*S*-(EBI)$ZrCl_2$,[28] followed by subsequent conversions to (*S*,*S*)-(EBI)$ZrMe_2$ using Me_2Mg, to (*S*,*S*)-(EBI)ZrMe(OTf) using TMSOTf, to neutral methyl ester enolate precatalyst (*S*,*S*)-(EBI)ZrMe[OC(O^{i}Pr)=CMe_2] {(*S*,*S*)-pre-**1**, $[\alpha]^{23}_D$ = +290°, *c* = 0.49 g/dL, CH_2Cl_2} using Li(IPIB), and finally to cationic ester enolate catalyst (*S*,*S*)-(EBI)Zr$^+$(THF)[OC(O^{i}Pr)=CMe_2][MeB-$(C_6F_5)_3$]$^-$ {(*S*,*S*)-**1**, $[\alpha]^{23}_D$ = −69.7°, *c* = 0.98 g/dL, CH_2Cl_2} using $(C_6F_5)_3B\cdot$THF. The procedures for the last four steps were identical to those already published for the racemic diastereomers, including the methylation step[29] and the final three steps.[19,30] The synthesis of the (*R*,*R*) enantiomer follows the identical procedures for the

Scheme 1. Outlined Overall Synthesis of Enantiomeric Catalysts (*S*,*S*)-1 and (*R*,*R*)-1

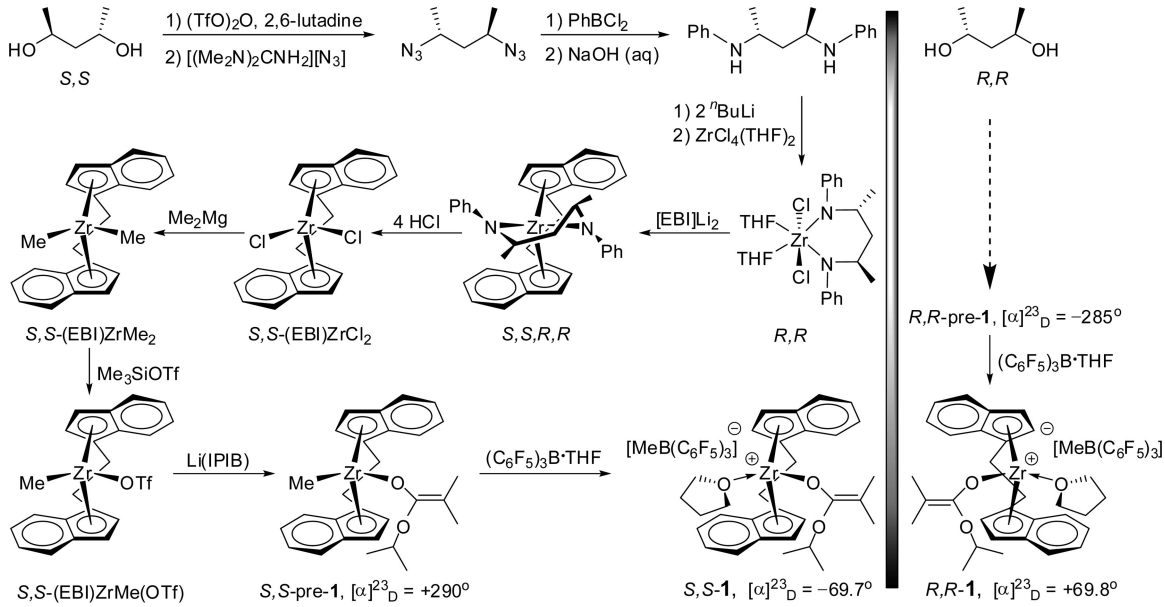

(*S*,*S*) enantiomer, leading to neutral methyl ester enolate precatalyst (*R*,*R*)-(EBI)ZrMe[OC(O^{i}Pr)═CMe$_2$] (*R*,*R*-pre-**1**, $[\alpha]^{23}_D = -285°$, $c = 0.49$ g/dL, CH_2Cl_2) and last cationic ester enolate catalyst (*R*,*R*)-(EBI)Zr$^+$(THF) [OC(O^{i}Pr)═CMe$_2$][MeB(C$_6$F$_5$)$_3$]$^-$ {(*R*,*R*)-**1**, $[\alpha]^{23}_D = +69.8°$, $c = 0.98$ g/dL, CH_2Cl_2 after methide abstraction by (C$_6$F$_5$)$_3$B·THF. The spectroscopic data for enantiomeric **1** are identical to those already reported for *rac*-**1**.[19] It is worth noting that in the step of the preparation of dimethyl zirconocenes (*S*,*S*)-(EBI)ZrMe$_2$ and (*R*,*R*)-(EBI)ZrMe$_2$, the ether-solvated magnesium salt coproducts were inseparable from the desired dimethyl complexes by repeated recrystallization from various solvents or filtration over Celite; however, treatment of the crude product mixture under high vacuum (10^4−10^6 torr) at 80 °C for 6 h, followed by dissolution of the residue in toluene, filtration, and drying of the filtrate in vacuo afforded the clean dimethyl complexes.

General Polymerization Procedures. Polymerizations were performed in 30-mL glass reactors inside the glovebox for the reactions carried out at ambient temperature (~23 °C). In a typical procedure for homopolymerization, predetermined amounts of B(C$_6$F$_5$)$_3$·THF and the appropriate precatalyst in a 1:1 molar ratio were premixed in 5 mL of CH_2Cl_2 and stirred for 10 min to cleanly generate the corresponding cationic catalyst.[20] A monomer was quickly added either as a solid or by pipet to the vigorously stirring solution, and the reaction was allowed to proceed for 3 h with continuous stirring. Polymerizations of DIPA and APY, which did not occur at ambient temperature, were carried out at 80 °C and performed in 25-mL Schlenk flasks equipped with stir bar and septum cap. Predetermined amounts of B(C$_6$F$_5$)$_3$·THF and the appropriate precatalyst were dissolved in 5 mL of 1,2-dichlorobenzene and stirred for 10 min at ambient before addition of monomer. Thereafter, the charged Schlenk flask was taken out of the glovebox and immersed in an oil bath that was pre-equilibrated at 80 °C, and the reaction proceed for 1 h with vigorous stirring. After the measured time interval, a 0.2 mL aliquot was taken from the reaction mixture via syringe and quickly quenched into a 4 mL vial containing 0.6 mL of undried "wet" $CDCl_3$ stabilized by 250 ppm of BHT-H; the quenched aliquots were later analyzed by ^{1}H NMR to obtain monomer conversion data. The polymerization was immediately quenched after the removal of the aliquot by addition of 5 mL of 5% HCl-acidified methanol. The quenched mixture was precipitated into 100 mL of methanol, stirred for 1 h, filtered or centrifuged, washed with methanol, and dried in a vacuum oven at 50 °C overnight to a constant weight. P(DMAA) and P(APY) were precipitated into 100 mL of diethyl ether and stirred for 1 h. The product was obtained as a sticky solid and dried in a vacuum oven at 50 °C overnight to a constant weight; the polymer was redissolved in a minimum of methylene chloride, precipitated into a 10-fold excess of diethyl ether, stirred for 1 h, filtered, washed with diethyl ether, and dried in a vacuum oven at 50 °C overnight to a constant weight.

The amounts of the monomers employed for the polymerizations are listed as follows. DPAA, 4.48 mmol; PTAA, 0.85 mmol; HPAA, 0.39 mmol; MPAA, 3.10 mmol; DIPA, 3.22 mmol; APY, 4.25 mmol; APP, 3.7 mmol; PAA, 1.36 mmol; EAA, 2.0 mmol; DMMA, 9.34 mmol; MMA, 9.34 mmol; BMA, 9.34 mmol; and EHM, 9.34 mmol. The amount of the precatalyst, in combination with 1 equiv of the activator B(C$_6$F$_5$)$_3$·THF, was adjusted according to the [monomer]/[catalyst] ratio specified in the polymerization tables. For block copolymerizations of MMA with a second monomer, after in situ generation of the catalyst in the identical fashion as described above, 400 equiv of MMA was quickly added via pipet and vigorously stirred for 10 min (for a quantitative MMA conversion) before the addition of the second monomer. The polymerization of the second monomer proceeded for 3 h with continuous stirring.

Kinetics of DPAA Polymerization. Kinetic experiments for the polymerization of DPAA were carried out in 30 mL reactors inside of the glovebox at ambient temperature (~23 °C) using a similar procedure as that already described above, except that, at appropriate time intervals, 0.2 mL aliquots were withdrawn from the reaction mixture using a syringe and quickly quenched into 1 mL septum cap sealed vials containing 0.6 mL of undried "wet" $CDCl_3$mixed with 250 ppm of BHT-H. The quenched aliquots were analyzed by ^{1}H NMR to determine monomer conversions. Specifically, predetermined amounts of B(C$_6$F$_5$)$_3$·THF and *rac*-**1** in a 1:1 molar ratio were premixed in 5 mL of CH_2Cl_2 and stirred for 10 min before 2.24 mmol DPAA was added as a solid. Owing to the insolubility of P(DPAA), 0.746 mmol toluene was added to the reaction solution to act as an internal standard and the percent of the unreacted DPAA at a given time t, was determined by integration of the peaks for DPAA (6.5 ppm for one of the vinyl protons) and toluene (2.09 ppm for the methyl protons) according to the percent of unreacted DPAA $= (\mathbf{A}_{6.5}/\mathbf{A}_{2.09}) \times 100$, where $\mathbf{A}_{6.5}$ is the total integrals for the peaks centered at 6.5 ppm and $\mathbf{A}_{2.09}$ is the total integral for the peak centered at 2.09 ppm. Apparent rate constants (k_{app}) were extracted by linearly fitting a line to the plot of $\ln([DPAA]_0/[DPAA]_t)$ vs time t. The polymerization became heterogeneous at high monomer conversions (the conversion at which the heterogeneity becomes apparent depends on the initial [DPAA]/[Zr] ratio employed), which eliminated the ability to

perform the NMR analysis of the aliquots taken at higher monomer conversions.

Polymer Characterizations. Gel permeation chromatography (GPC) and light scattering (LS) analyses of the polymers were carried out at 40 °C and a flow rate of 1.0 mL/min, with $CHCl_3$ as the eluent, on a Waters University 1500 GPC instrument coupled with a Waters RI detector and a Wyatt miniDAWN Treos LS detector. The GPC instrument is equipped with one PLgel 5 μm guard and three PLgel 5 μm mixed-C columns (Polymer Laboratories; linear range of molecular weight = 200–2 000 000), and calibrated with 10 P(MMA) standards. Chromatograms were processed with Waters Empower software (version 2002); number-average molecular weight (M_n) and polydispersity (M_w/M_n) of polymers were given relative to P(MMA) standards. Weight-average molecular weight (M_w) was obtained from the analysis of the LS data which was processed with Wyatt Astra Software (version 5.3.2.15), and d*n*/d*c* values were determined assuming 100% mass recovery of polymers with known concentrations. The insoluble P(DPAA) samples produced by *rac*-**1** were converted to the $CHCl_3$-soluble poly(methyl acrylate) derivative for their GPC analysis, using literature procedures.[14a]

Maximum rate decomposition temperatures (T_{max}) and decomposition onset temperatures (T_{onset}) of the polymers were measured by thermal gravimetric analysis (TGA) on a TGA 2950 Thermogravimetric Analyszer, TA Instrument. Polymer samples were heated from ambient temperatures to 600 °C at a rate of 20 °C/min. Values for T_{max} were obtained from derivative (wt %/°C) vs temperature (°C), while T_{onset} values (initial and end temperatures) were obtained from wt % vs temperature (°C) plots.

Optical rotations were measured on an Autopol III Automatic Polarimeter at 23 °C. The measurements were conducted on 0.2 g/dL polymer solutions, 0.49 g/dL enantiomeric precatalyst solutions, and 0.98 g/dL enantiomeric cationic catalyst solutions. Polymer samples were dissolved in $CHCl_3$ except homopolymer P(DPAA), P(PTAA), P(MPAA), and P(APP) samples which were dissolved in $CHCl_3$ with addition of a small amount of CF_3COOH,[14a] and the enantiomeric catalysts in CH_2Cl_2. On the basis of multiple measurements on selected polymer samples, the errors associated with specific rotations of the chiral polymer solutions range from 5% to 10%, depending on the magnitude of the specific rotation values. Circular dichroism (CD) spectra were obtained from an Aviv model 202 CD spectrometer. CD analysis was conducted on polymer solutions with concentrations of 0.2 g/dL. Block copolymers were dissolved in THF, while homopolymers were dissolved in $CHCl_3$, except P(DPAA), P(PTAA), P(MPAA), and P(APP) samples which were dissolved in $CHCl_3$ with addition of a small amount of CF_3COOH.

Results and Discussion

Kinetics of DPAA Polymerization. Our previous mechanistic studies have demonstrated that the coordination polymerization of *N*,*N*-dialkyl acrylamide DMAA by *rac*-**1** proceeds in a monometallic, site-control, coordination-conjugate addition mechanism through eight-membered-ring cyclic amide enolate intermediates (i.e., structure **A**, Scheme 2).[21] The resting state during a "catalytic" propagation cycle is the cyclic amide enolate **A** and associative displacement of the coordinated penultimate amide group by incoming acrylamide monomer to regenerate the active species is the rate-determining step, giving rise to the propagation kinetics that is first order in both concentrations of the monomer and the catalyst.

To examine if the polymerization of *N*,*N*-diaryl amides follows the same scheme established for *N*,*N*-dialkyl amides, kinetics of the DPAA polymerization by *rac*-**1** was investigated, the results of which are summarized in Figure 1. The kinetic experiments employed the $[DPAA]_0/[rac\text{-}\mathbf{1}]_0$ ratios ranging from 50 to 400; however, insolubility of the polymer hampered the efforts to perform accurately the NMR analysis of the aliquots taken at high conversions for the larger $[DPAA]_0/[rac\text{-}\mathbf{1}]_0$ ratio

Scheme 2. Proposed Initiation and Propagation Steps in the Polymerization of Acrylamides by *rac*-1

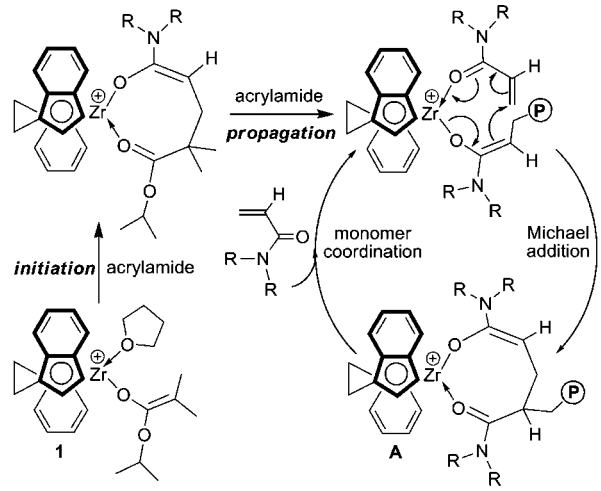

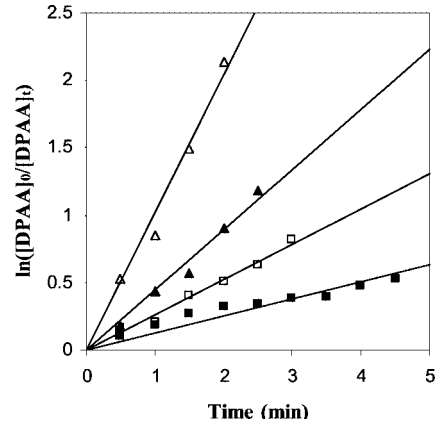

Figure 1. Semilogarithmic plots of $\ln([DPAA]_0/[DPAA]_t)$ vs time for the polymerization of DPAA by *rac*-**1** in CH_2Cl_2 at ambient temperature (~23 °C). Conditions: $[DPAA]_0 = 0.448$ M; $[rac\text{-}\mathbf{1}]_0 = 8.95$ mM (Δ), 4.47 mM (▲), 2.24 mM (□), 1.12 mM (■).

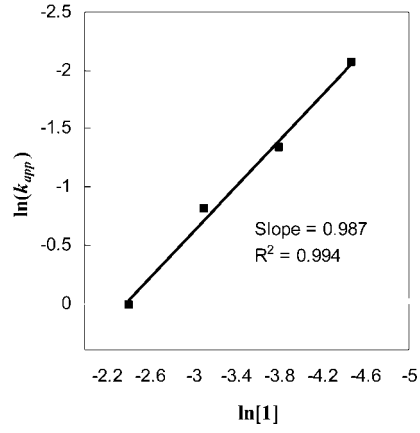

Figure 2. Plot of $\ln(k_{app})$ vs ln[**1**] for the DPAA polymerization by *rac*-**1** in CH_2Cl_2 at ambient temperature.

runs. Nevertheless, the available data collected clearly show that propagation is first order in [DPAA] for all the $[DPAA]_0/[rac\text{-}\mathbf{1}]_0$ ratios investigated in this study (Figure 1). Furthermore, a double logarithm plot (Figure 2) of the apparent rate constants (k_{app}), obtained from the slopes of the best-fit lines to the plots of $\ln([DPAA]_0/[rac\text{-}\mathbf{1}]_0)$ vs time, as a function of $\ln[rac\text{-}\mathbf{1}]_0$ was fit to a straight line ($R^2 = 0.994$) of slope 0.987. Thus, the kinetic order with respect to [*rac*-**1**], given by the slope of ~1 (0.987),

Table 1. Selected Results of Polymerization of *N*,*N*-Diaryl Acrylamides by 1[a]

run no.	monomer	[monomer] /[1]	Catalyst form	yield[b] (conv)	10^4 M_w[c] (g/mol)	MWD[c] (M_w/M_n)	$[\alpha]^{23}_D$[d] (deg)
1	DPAA	200	*rac*	97	3.97	1.03	
2	DPAA	50	*rac*	96	1.16	1.13	0.0
3	DPAA	50	*S*,*S*	96			−15.5
4	DPAA	50	*R*,*R*	96			+19.5
5	PTAA	50	*rac*	(100)			0.0
6	PTAA	50	*S*,*S*	(100)			−159
7	PTAA	50	*R*,*R*	(100)			+180
8	HPPA	50	*S*,*S*	(100)	19.8	1.25	+152
9	HPPA	50	*R*,*R*	(100)	18.1	1.38	−161

[a] Carried out in 5 mL of CH_2Cl_2 at ambient temperature for 3 h. [b] Isolated polymer yield or monomer conversion in parenthesis, (conv), measured by ^{1}H NMR. [c] Determined by GPC relative to P(MMA) standards for runs 1 and 2 which were based on the poly(methyl acrylate) derivatives, or by LS for runs 8 and 9. [d] Determined by polarimetry (c = 2 g/dL in $CHCl_3$; DPAA and PTAA polymer samples were dissolved in $CHCl_3$ with a small amount of CF_3COOH, while HPPA polymer samples were dissolved in $CHCl_3$ only.

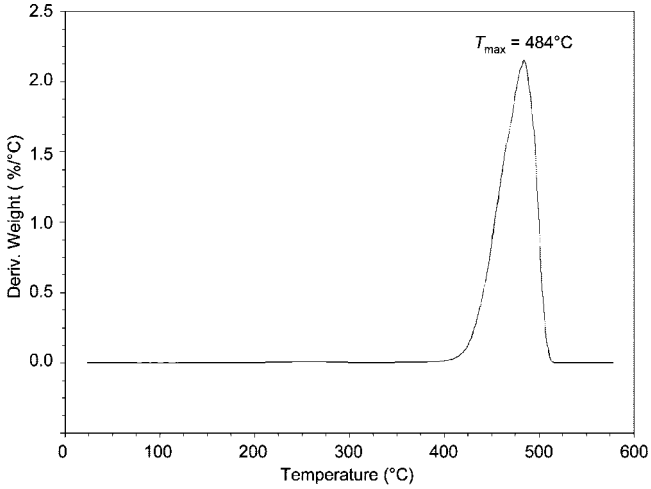

Figure 3. TGA derivative plot of P(DPAA) produced by *rac*-**1** (run 1, Table 1).

reveals that the propagation is also first order in catalyst concentration, indicating that the *N*,*N*-diaryl amide polymerization catalyst **1** follows the same mechanism as that of the *N*,*N*-dialkyl amide polymerization shown in Scheme 2.

Polymerization of *N*,*N*-Diaryl Acrylamides. Racemic catalyst **1** was initially employed to examine the catalyst reactivity toward *N*,*N*-diaryl acrylamides for rendering solution-stable helical conformations of the corresponding highly isotactic polymers. Thus, polymerization of 50 and 200 equiv of DPAA in CH_2Cl_2 at ambient temperature using *rac*-**1** proceeds to quantitative monomer conversions (although the reaction started to become heterogeneous after ~5 min), affording P(DPAA) (runs 1 and 2, Table 1) with a high T_{max} (maximum-rate-decomposition temperature) of 484 °C in a narrow, one-step decomposition window (Figure 3). The rigid helical structure of highly isotactic P(DPAA)[14] can be viewed in the space-filing model of the most stable conformation as a 5_1 helix (Figure 4); the P(DPAA) produced by the highly isospecific coordination catalyst *rac*-**1** is also insoluble in common organic solvents, precluding its direct MW measurements by GPC. Accordingly, it was converted to the soluble poly(methyl acrylate) derivative by treatment with concentrated H_2SO_4 in MeOH at 90 °C for 24 h, followed by methylation with CH_2N_2.[14] The measured MW and MWD (M_w = 3.97 × 10^4, M_w/M_n = 1.03 and M_w = 1.16 × 10^4, M_w/M_n = 1.13 for $[DPAA]_0/[rac\text{-}1]_0$ = 200 and 50, respectively) of the poly(methyl acrylate) derivative (runs

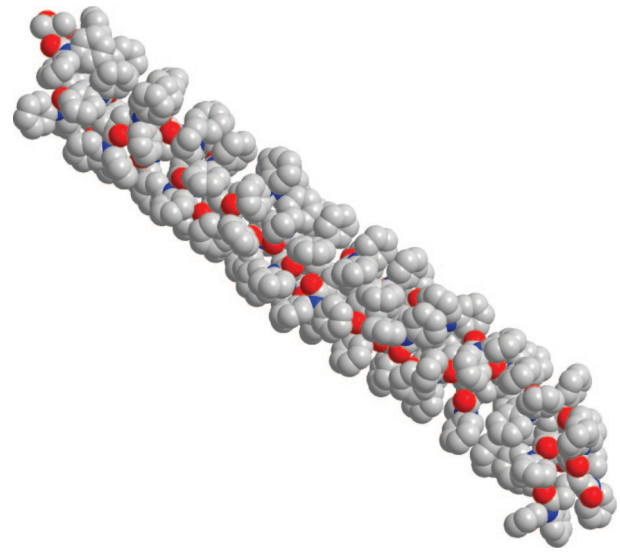

Figure 4. MM2-calculated 5_1 helical structure of a 50-mer of isotactic P(DPAA) viewed as a space-filling model (carbon, nitrogen, and oxygen are grey, blue, and red, respectively; H atoms omitted).

1 and 2, Table 1) demonstrate the controlled/living nature of the DPAA polymerization.

Subsequently, we polymerized DPAA with enantiomeric catalysts (*R*,*R*)-**1** and (*S*,*S*)-**1**, successfully affording optically active P(DPAA)s with excess one-handed helicity (runs 3 and 4, Table 1). Thus, the enantiomeric catalysts produce polymers of approximately opposite specific rotation to one another (see Experimental Section for error information): $[\alpha]^{23}_D$ = −15.5° by (*S*,*S*)-**1**, $[\alpha]^{23}_D$ = +19.5° by (*R*,*R*)-**1**, showing the enantiomeric nature of the resulting polymers and determination of the handedness of the polymer helix by the configuration of the enantiomeric catalyst used. Furthermore, the P(DPAA) also exhibits opposite optical rotation to those of the respective neutral catalyst precursors used. Although the optically active P(DPAA) shows the same sign of optical rotation as that of each enantiomeric cationic zirconocenium catalyst, the possibility of the observed optical activity could arise from the catalyst residue in its cationic form is eliminated by the careful removal of the catalyst residue during postpolymerization workup procedures (see Experimental Section), by circular dichroism (CD) analysis that the catalyst did not exhibit any absorption peaks in the region observed for the polymer (vide infra), and also by control experiments that optically inactive, nonhelical, high-MW polymers such as P(DMAA) and P(MMA) produced by either (*R*,*R*)-**1** or (*S*,*S*)-**1** always gave zero values by polarimetry, following the same postpolymerization workup procedures, which confirms the complete removal of the catalyst or ligand residue using our procedure.

We also examined the possible modulation on optical activity of the polymer by unsymmetrical substitution of the phenyl groups of poly(*N*,*N*-diary acrylamide)s. To this end, we extended this asymmetric coordination polymerization system to *N*-phenyl-*N*-(4-tolyl)acrylamide (PTAA). Specifically, polymerizations of PTAA by *rac*-**1**, (*S*,*S*)-**1**, and (*R*,*R*)-**1** are as effective as the DPAA polymerization, producing rigid helical P(PTAA) whose optical activity and screw-sense helices are determined by the form of the catalyst employed—$[\alpha]^{23}_D$ = 0.0°, −159°, and +180° by *rac*-**1**, (*S*,*S*)-**1**, and (*R*,*R*)-**1**, respectively (runs 5–7, Table 1). These results were further confirmed by their CD spectra (Figure 5) which show no, positively signed, or negatively signed Cotton effects in the characteristic region of a $\pi \rightarrow \pi^*$ transition of the phenyl ring in the P(PTAA) produced by *rac*-**1**, (*S*,*S*)-**1**, and (*R*,*R*)-**1**, respectively, and that the latter two are near mirror images of each other. Of significance here

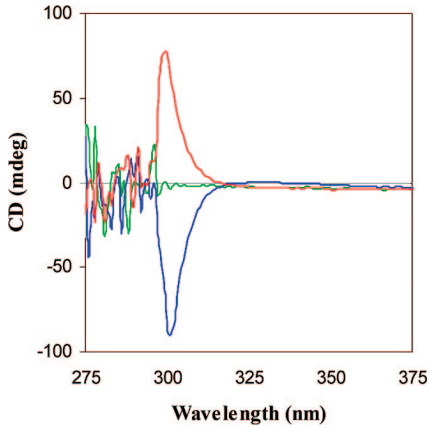

Figure 5. CD spectra ($CHCl_3$/CF_3COOH) of P(PTAA) produced by catalysts (*S*,*S*)-**1** (red), *rac*-**1** (green), and (*R*,*R*)-**1** (blue).

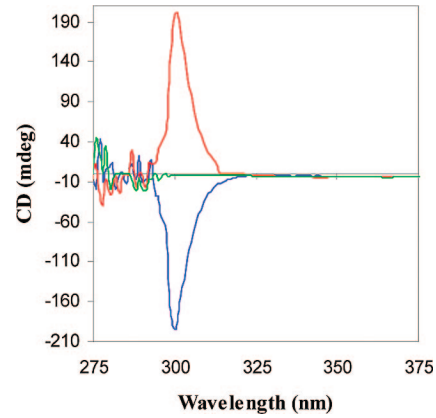

Figure 6. CD spectra ($CHCl_3$) of P(HPPA) produced by catalysts (*S*,*S*)-**1** (red), *rac*-**1** (green), and (*R*,*R*)-**1** (blue).

are the observed ~10 times higher specific rotation values for P(PTAA) than P(DPAA).

The stereoregular, rigid helical P(DPAA) and P(PTAA) produced are insoluble in common organic solvents, precluding their direct measurements of MW by GPC, as well as optical activity by polarimetry and CD in common solvents such as $CHCl_3$ (without addition of CF_3COOH). We reasoned that it would be possible for a polymer based on *N*-(4-hexylphenyl)-*N*-phenyl acrylamide (HPPA)[14a] to overcome this issue because the long-chain alkyl group on each repeat unit of the resulting polymer should enhance its solubility, and furthermore, the unsymmetrically substituted phenyl groups on N should give rise to the polymer with a large specific rotation [e.g., P(PTAA) vs P(DPAA)]. Accordingly, polymerization of 50 equiv of HPPA was performed by catalysts (*S*,*S*)-**1** and (*R*,*R*)-**1**, satisfactorily leading to the optically active, one-handed helical P(HPPA) that is soluble directly in $CHCl_3$ (runs 8 and 9, Table 1); polymers of higher MWs were found to be insoluble in $CHCl_3$. The measured absolute MWs by light scattering are ~10 times higher than the calculated value strictly based on the monomer to catalyst feed ratio, likely due to association of the chains. Again, the enantiomeric catalysts produced P(HPPA)s of opposite specific rotation, but interestingly, the specific rotations of these polymers are opposite in sign to that of P(DPAA) or P(PTAA) produced by the same enantiomeric catalysts. It is currently unclear why there is alteration in sign of specific rotation, but it is important to note that these results do not give insight into the handedness of the helix, although it is assumed that the handedness of P(HPPA) is the same as that of P(DPAA) or P(PTAA) produced by the same enantiomeric catalysts due to the enantiomorphic site-control mechanism of the polymerization. Indeed, the CD analysis of the P(HPPA) produced by *rac*-**1**, (*S*,*S*)-**1**, and (*R*,*R*)-**1** showed no, positively signed, and negatively signed Cotton effects, respectively (Figure 6), which is the same as what was observed for P(PTAA) (c.f. Figure 5). As in P(PTAA), P(HPPA) with two nonequivalent aryl groups on amide N (i.e., unsymmetrical substitution) shows much larger specific rotations as compared to P(DPAA) with symmetrical substitution.

Block Copolymerization of *N*,*N*-Diaryl Acrylamides with MMA. The following three reasons prompted us to investigate the block copolymerizations of MMA with DPAA and PTAA: (a) use of a large MMA block to help solubilize the rigid helical acrylamide block, (b) further confirmation of the living/controlled nature of this polymerization system, and (c) production of the unique optically active, flexible random coil−rigid helical block copolymers. The block copolymerizations were carried out in a ratio of [MMA]/[acrylamide][**1**] = 400:50:1 at ambient temperature by starting the polymerization of MMA first, the results of which are summarized in Table 2.

Indeed, block copolymers $P(MMA)_{400}$-*b*-$P(DPAA)_{50}$ and $P(MMA)_{400}$-*b*-$P(PTAA)_{50}$ are soluble in $CHCl_3$, but the measured absolute MWs by light scattering are substantially higher than the calculated value strictly based on the monomer-to-catalyst-feed ratio, likely due to the association of the polymer chains such as micelle formation. (The subscripted numbers shown in the block copolymer formula represent only the comonomer feed, and they do not necessarily or precisely reflect on copolymer composition.) Significantly, the block copolymers produced have narrow, unimodal MW distributions of M_w/M_n = 1.07–1.21, further confirming the living/controlled nature of the present polymerization system. The block copolymer composition is confirmed by TGA analysis (Figure 7) which showed 20 wt % for the P(DPAA) block in the block copolymer as compared to the calculated 18 wt % on the basis of $P(MMA)_{400}$-*b*-$P(DPAA)_{50}$ or the monomer feed ratio. The optical activity of these block copolymers also hinges on the nature of the catalyst although, as expected, the specific rotation value of the block copolymer is much smaller than the respective homopolymer because of the weight fraction contribution of the large, optically inactive P(MMA) block; while *rac*-**1** afforded the optically inactive copolymer (runs 10 and 13, Table 2), (*S*,*S*)-**1** and (*R*,*R*)-**1** led to the copolymers of opposite optical rotation (runs 11 and 14 vs runs 12 and 15, Table 2). These results were further confirmed by their CD spectra (Figures 8 and 9) which show no, positively signed, and negatively signed Cotton effects for the block copolymers produced by *rac*-**1**, (*S*,*S*)-**1**, and (*R*,*R*)-**1**, respectively.

Effects of Chain Length on Optical Activity of Helical Poly(acrylamide)s. Because of the cryptochiral phenomenon of stereoregular vinyl polymers, only those low-MW, enantiomeric oligomers exhibit measurable optical activity in solution, and the optical activity of such oligomers *increases* with a *decrease* in MW due to chain-end group effects (vide supra). However, the optical activity of the rigid helical poly(*N*,*N*-diaryl acrylamide)s of the current study does not rely on chain-end groups to eliminate reflection elements of symmetry, but rather by secondary structure of stable helical conformation. Intuitively, as the chain length of such polymers increases and the helical structure becomes more pronounced, the optical activity should rise. Thus, at shorter chain lengths the helix may not be fully developed, resulting in lower optical activity, and chain-end group effects on the chiroptical properties of the polymer become more significant. To test this hypothesis, we conducted the PTAA polymerization varying the [PTAA]/[(*R*,*R*)-**1**] ratio. The insolubility of the resulting P(PTAA) in common organic solvents prevented its direct MW analysis; thus, interpretation of the specific rotations of these polymers as a function of MW

Table 2. Results of Block Copolymerization of MMA with *N*,*N*-Diaryl Acrylamides by 1[a]

run no.	comonomer	[M]/[co-M] /[**1**]	catalyst form	yield (%)	10^4 M_w[b] (g/mol)	MWD[b] (M_w/M_n)	$[\alpha]^{23}_D$[c] (deg)
10	DPAA	400:50:1	*rac*	>99	376	1.19	0.0
11	DPAA	400:50:1	*S*,*S*	>99	358	1.15	−8.5
12	DPAA	400:50:1	*R*,*R*	>99	264	1.21	+11.0
13	PTAA	400:50:1	*rac*	>99	103	1.08	0.0
14	PTAA	400:50:1	*S*,*S*	>99	111	1.09	−27.0
15	PTAA	400:50:1	*R*,*R*	>99	123	1.07	+32.0

[a] Carried out in 5 mL of CH_2Cl_2 at ambient temperature for 10 min of MMA polymerization followed by 3 h of acrylamide polymerization. [b] Determined by LS. [c] Specific rotation measured in $CHCl_3$.

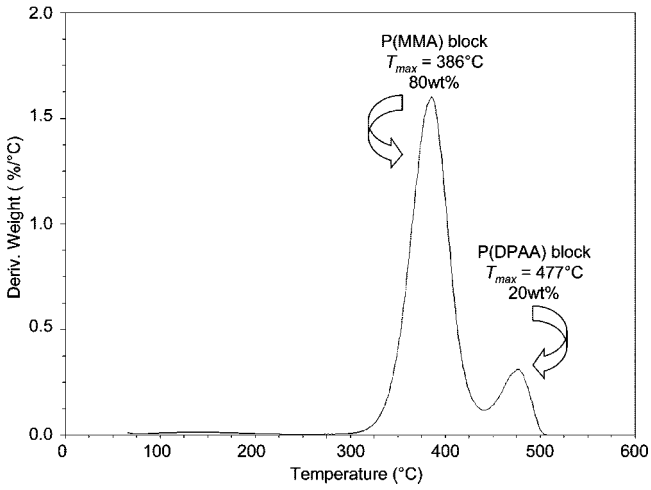

Figure 7. TGA derivative plot of $P(MMA)_{400}$-*b*-$P(DPAA)_{50}$ produced by (*S*,*S*)-**1** (run 11 in Table 2).

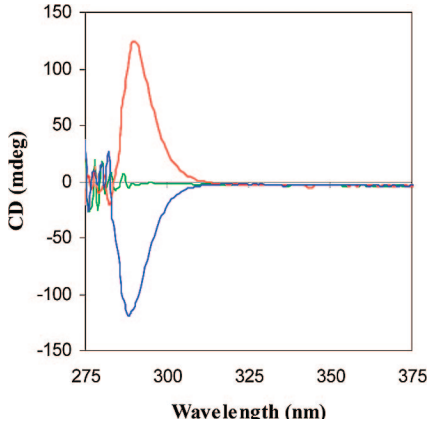

Figure 8. CD spectra (THF) of $P(MMA)_{400}$-*b*-$P(DPAA)_{50}$ produced by catalysts (*S*,*S*)-**1** (red), *rac*-**1** (green), and (*R*,*R*)-**1** (blue).

(chain length) was based on the [PTAA]/[(*R*,*R*)-**1**] ratio employed because the controlled nature of this polymerization system was confirmed by other means (vide supra). As depicted in Figure 10, the specific rotation of the chiral polymer solution (in $CHCl_3$ with addition of a small amount of CF_3COOH) indeed increases with an increase in the monomer feed ratio (and thus the polymer chain length). Of significance, when the [PTAA]/[(*R*,*R*)-**1**] ratio is increased from 20 to 30 there is an enormous climb in the $[\alpha]^{23}_D$ value by 113.2 °! This large increase in specific rotation between these two ratios may correspond to the formation of a well-defined helix and multiple turns in the helix for the polymers synthesized with [PTAA]/[(*R*,*R*)-**1**] > 20. In comparison, when the [PTAA]/[(*R*,*R*)-**1**] ratio is increased from 30 to 50, there is a much smaller increase in specific rotation by 32.0°. We presently do not know, however, the maximum specific rotation of this polymer can achieve because higher MW P(PTAA)s become insoluble in $CHCl_3/CF_3COOH$, precluding their solution specific rotation measurements.

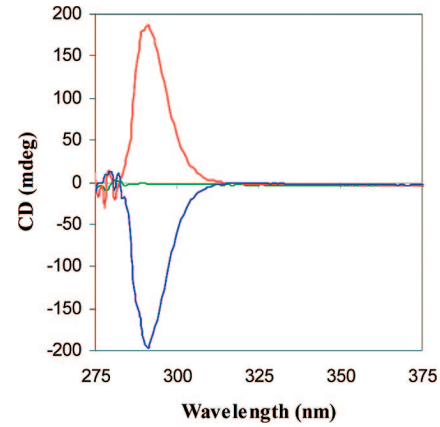

Figure 9. CD spectra (THF) of $P(MMA)_{400}$-*b*-$P(PTAA)_{50}$ produced by catalysts (*S*,*S*)-**1** (red), *rac*-**1** (green), and (*R*,*R*)-**1** (blue).

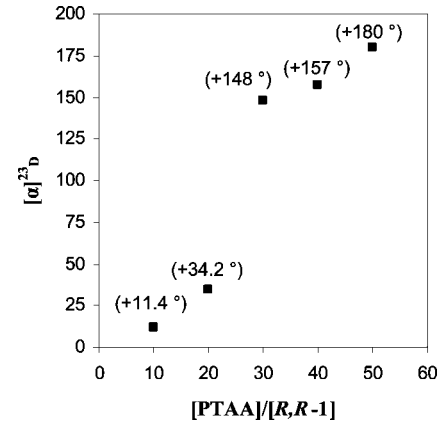

Figure 10. Plot of specific rotation $[\alpha]^{23}_D$ values of P(PTAA) vs the [PTAA]/[(*R*,*R*)-**1**] ratio employed.

Table 3. Results of Polymerization of *N*-(4-Hexylphenyl)-*N*-phenyl Acrylamide (HPPA) by (*R*,*R*)-1

run no.	[HPPA]/[**1**]	conv (%)	10^4 M_w[a] (g/mol)	MWD[a] (M_w/M_n)	$[\alpha]^{23}_D$[b] (deg)
16	10	>99	1.04	1.00	+1.5
17	20	>99	2.16	1.01	−7.8
18	30	>99	4.65	1.23	−11.0
19	40	>99	7.74	1.75	−67.6
20	50	>99	18.1	1.38	−161

[a] Determined by LS. [b] Specific rotation measured in $CHCl_3$.

The use of soluble low-MW P(HPPA) in $CHCl_3$ allowed establishing a direct plot between MW and optical activity. To this end, five P(HPPA) samples were prepared from the polymerization using the [HPPA]/[(*R*,*R*)-**1**]) ratio = 10, 20, 30, 40, and 50 to produce the corresponding polymers with their absolute M_w and MWD measured by LS, as well as specific rotations measured by polarimetry in $CHCl_3$ being summarized in Table 3. Again, the measured specific rotation (absolute value) of the chiral polymer increases with an increase in the polymer MW (chain length), Figure 11. However, surprisingly, the lowest

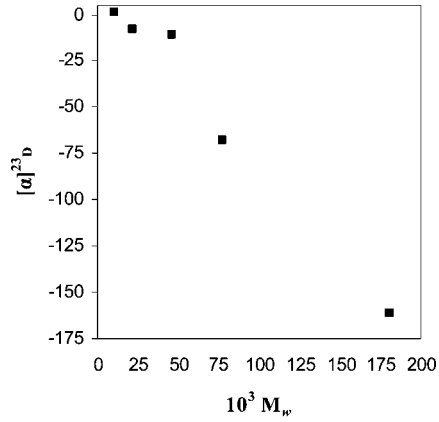

Figure 11. Plot of specific rotation $[\alpha]^{23}_D$ values of P(HPPA) produced by (*R*,*R*)-**1** vs M_w.

Table 4. Selected Results of Polymerization of Non-Diaryl Acrylamides by (*R*,*R*)-1[a]

run no.	M/co-M	[M]/[co-M /[**1**]	yield (conv)	10^4 M_w[b] (g/mol)	MWD[b] (M_w/M_n)	$[\alpha]^{23}_D$[c] (deg)
21	MPAA	50:1	97			+0.9
22	MPAA	30:1	(100)			+1.7
23	MPAA	10:1	(100)			+6.6
24	MPAA/MMA	50:400:1	(100)	21.2	1.01	+4.8
25	DMAA	50:1	>99			+6.0
26	DMAA	400:1	>			0.0
27	DMAA/MMA	400:400:1	>99			+5.5
28	DMAA/MPAA	400:100:1	>99			+6.3
29	DIPA/MMA	50:400:1	(100)	18.8	1.01	+2.7
30	APP	50:1	(100)			+3.1
31	APP/MMA	50:400:1	(100)	10.0	1.29	+6.0

[a] Carried out in 5 mL of CH_2Cl_2 at ambient temperature for 10 min (for MMA and DMAA) or 3 h (for MPAA or APP), or in 5 mL of *o*-$C_6H_4Cl_2$ at 80 °C for 1 h (for DIPA and APY). [b] Determined by LS. [c] Specific rotation measured in $CHCl_3$ for block copolymers and DMAA homopolymers or in $CHCl_3$ with addition of a small amount of CF_3COOH for MPAA and APP homopolymers.

MW polymer sample showed a small, but positive, specific rotation, whereas when the MW of P(HPPA) further increased the specific rotation became largely negative. This observation is most likely an effect of helix formation in that the small MW polymer does not fully develop the solution-stable helix, and thus, optical activity arises chiefly from the chirality in the main chain and nonequivalent chain-end groups; with further increasing MW the helix is more defined so that specific rotation is of the same sign for the polymers of the same screw sense and also becomes more largely negative with an increase in MW (Figure 11).

Polymerization of Non-Diaryl Acrylamides. The above success in converting prochiral *N*,*N*-diaryl acrylamides to optically active, rigid helical polymers via asymmetric coordination polymerization brought forth a fundamental question of whether two aryl groups on amide N are of necessity in rendering a solution-stable helical conformation. To answer this question, we investigated polymerizations of seven non-diaryl acrylamides by systematic replacement of one or both phenyl groups on N with H or alkyl groups of varying steric hindrance (see Chart II for structures), including *N*-aryl-*N*-alkyl acrylamide MPAA, *N*-aryl acrylamide PAA, *N*-alkyl acrylamide EAA, *N*,*N*-dialkyl acrylamides DMAA and DIPA, and *N*,*N*-cyclic $(CH_2)_n$ acrylamides APY (n = 4) and APP (n = 5). Selected polymerization results are summarized in Table 4.

Polymerizations of these nondiaryl acrylamides were first examined using *rac*-**1** to determine their reactivity toward the current catalyst system and also serve as comparative examples when analyzing the results by the enantiomeric catalysts. All

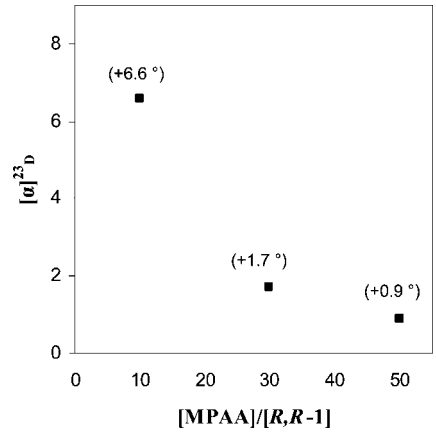

Figure 12. Plot of specific rotation $[\alpha]^{23}_D$ values of P(MPAA) vs the [MPAA]/[(*R*,*R*-**1**)] ratio.

homopolymers or block copolymers produced by *rac*-**1** gave zero readings in polarimetry as expected, and these results were not included in Table 4. P(MPAA) produced by (*R*,*R*)-**1** showed a small specific rotation of +0.9° (run 21, Table 4) in a [MPAA]/[(*R*,*R*)-**1**] ratio of 50; the polymer was almost cryptochiral on the basis of the $[\alpha]^{23}_D$ values and also exhibited no Cotton effects from its CD analysis, implying that a helical structure was not formed. A further study of effects of the [MPAA]/[(*R*,*R*)-**1**] ratio on optical activity of the resulting polymer (runs 21–23, Table 4) confirmed the above conclusion. Thus, in sharp contrast to the optically active, rigid helical poly(*N*,*N*-diaryl acrylamide)s, a decrease in the MPAA monomer feed ratio (thus the polymer chain length) increases the specific rotation of the polymer (Figure 12), characteristic of the small optical activity due to configurational chirality relied on chain-end group effects rather than helically conformational chirality (vide supra). A block copolymer of 50 equiv of MPAA with 400 equiv of MMA (run 24, Table 4) was also prepared to enable MW analysis and examination of optical activity of the copolymer. Interestingly, the enantiomeric copolymer $P(MMA)_{400}$-*b*-$P(MPAA)_{50}$ produced by (*R*,*R*)-**1** had a specific rotation of +4.8°, which is *much larger than* the specific rotation (+0.9°) of P(MPAA) synthesized using the same amount of MPAA. This observation is again contrary to all prior observations made for helical *N*,*N*-diaryl acrylamide−random coil MMA block copolymers, further supporting the conclusion that MPAA with only one phenyl group on N cannot produce a polymer with solution-stable helicity. Impressively, MM2 modeling of P(MPAA) drew the same conclusion (i.e., a random-coil structure, Figure 13).

Consistent with the inactivity of *rac*-**1** toward polymerization of *N*-isopropyl acrylamide (containing an acidic *N*−H proton) but high activity toward polymerization of DMAA,[21] catalyst (*R*,*R*)-**1** is unable to polymerize either PAA or EAA but rapidly polymerizes DMAA to isotactic P(DMAA) that exhibited a specific rotation of +6.0° in a [DMAA]/[(*R*,*R*)-**1**] ratio of 50 (run 25, Table 4). The enantiomeric P(DMAA) produced at a higher ratio of [DMAA]/[(*R*,*R*)-**1**] = 400 became cryptochiral (zero optical rotation, run 26, Table 4) as expected; however, the block copolymer $P(DMAA)_{400}$-*b*-$P(MMA)_{400}$ *is* optically active with $[\alpha]^{23}_D$ = +5.5° (run 27, Table 4), whereas each respective homopolymer of the same composition is cryptochiral. Likewise, the block copolymer $P(DMAA)_{400}$-*b*-$P(MPAA)_{100}$ *is* optically active with $[\alpha]^{23}_D$ = +6.5° (run 28, Table 4), whereas each respective homopolymer of the same composition is cryptochiral. These findings, along with the previously observed much larger optical activity of the block copolymer $P(MMA)_{400}$-*b*-$P(MPAA)_{50}$ than $P(MPAA)_{50}$, point to *an exciting strategy for producing optically active, nonhelical polymers via*

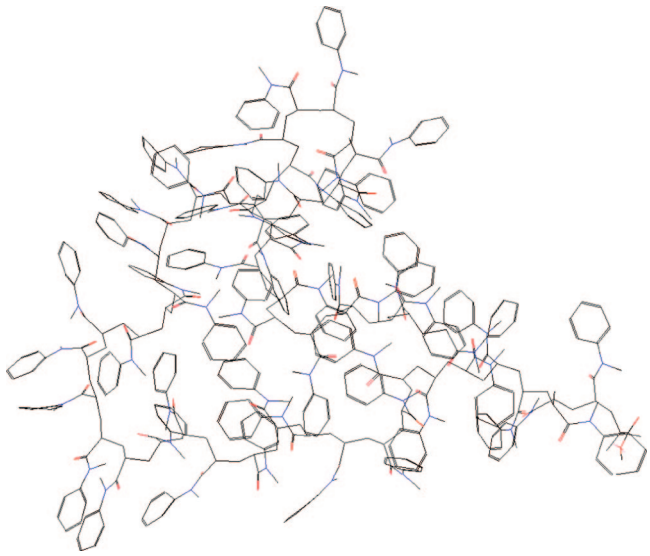

Figure 13. MM2-calculated random-coil structure of a 50-mer of isotactic P(MPAA) viewed as a wireframe model (carbon, nitrogen, and oxygen are grey, blue, and red, respectively; H atoms omitted).

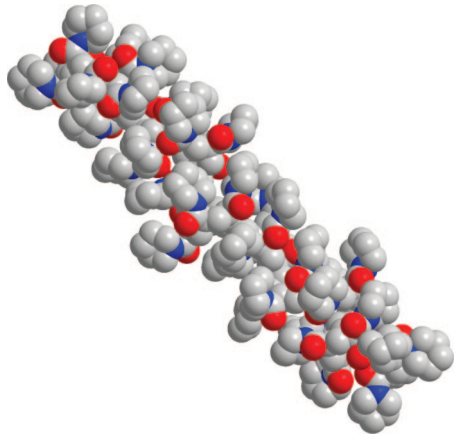

Figure 14. MM2-calculated approximately 6_1 helical structure of a 40-mer of chiral isotactic P(APP) viewed as a space-filling model (carbon, nitrogen, and oxygen are grey, blue, and red, respectively; H atoms omitted).

block copolymer formation. More discussion on this subject is described in next segment.

No polymerization occurred for DIPA or APY at ambient temperature; however, they were readily polymerized by catalyst **1** in *o*-dichlorobenzene at 80 °C (control runs without the catalyst showed no polymerization occurred at 80 °C up to 24 h). The resulting P(DIPA), with even a small [DIPA]/[(*R*,*R*)-**1**] ratio of 50 or 10, was insoluble in common solvents tested, inhibiting direct analysis of its optical activity. Subsequently, we synthesized the block copolymer $P(MMA)_{400}$-*b*-$P(DIPA)_{50}$ using (*R*,*R*)-**1** that showed a specific rotation of +2.7° (run 29, Table 4); the enantiomeric block copolymer was further analyzed by CD and showed no Cotton effects, implying that, like P(MPAA) and P(DMAA), it does not form a helical structure. P(APY) produced by (*R*,*R*)-**1** in a [APY]/[(*R*,*R*)-**1**] ratio of 200 is cryptochiral. However, according to MM2 modeling, the piperidine derivative APP would render a helical conformation (Figure 14). Accordingly, we polymerized APP using catalysts **1** achieving quantitative monomer conversions. The enantiomeric homopolymer P(APP) and block copolymer $P(MMA)_{400}$-*b*-$P(APP)_{50}$ exhibited small, but significant, specific rotations of +3.1° and +6.0°, respectively (runs 30 and 31, Table 4), initiating CD analysis for conformation of helical formation.

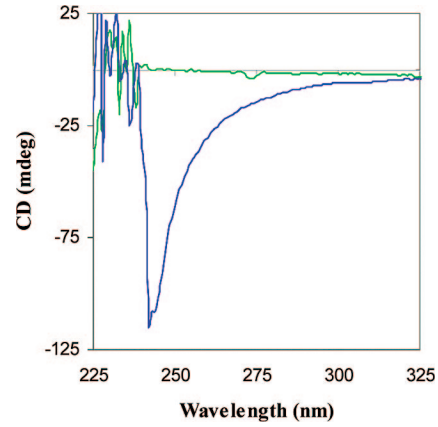

Figure 15. CD spectra ($CHCl_3/CF_3COOH$) of P(APP) by catalysts *rac*-**1** (green) and (*R*,*R*)-**1** (blue).

Table 5. Results of Polymerization of Methacrylates by 1[a]

run no.	M/co-M	catalyst form	yield (%)	$10^4 M_n$[b] (g/mol)	MWD[b] (M_w/M_n)	$[\alpha]^{23}_D$[c] (deg)
32	MMA	*R*,*R*	>99	0.66	1.05	+5.4
33	MMA	*R*,*R*	>99	1.07	1.03	+4.5
34	MMA	*R*,*R*	>99	2.56	1.05	+0.9
35	MMA	*R*,*R*	>99	3.01	1.05	0.0
36	BMA	*S*,*S*	>99	1.99	1.04	0.0
37	400MMA/400BMA	*S*,*S*	>99	16.3	1.07	0.0
38	400MMA/100BMA	*S*,*S*	89	8.93	1.04	0.0
39	400MMA + 400BMA	*S*,*S*	88	14.2	1.05	0.0
40	400MMA/400BMA/400EHM	*S*,*S*	>99	22.5	1.04	0.0

[a] Carried out in 5 mL of CH_2Cl_2 at ambient temperature for 10 min (MMA), 30 min (BMA), and 1 h (EHM). [b] Determined by GPC relative to P(MMA) standards. [c] Determined by polarimetry (c = 2 g/dL in $CHCl_3$).

Indeed, the CD spectra of P(APP) showed a large negative Cotton effect in the characteristic region of a $n \rightarrow \pi^*$ transition (Figure 15), thereby achieving the first chiral poly(*N*,*N*-*dialkyl*acrylamide) with solution-stable one-handed helicity.

To examine if the P(APP) produced by (*R*,*R*)-**1** with solution-stable one-handed helicity would racemize or not upon heating, we refluxed the P(APP) in $CHCl_3/CF_3COOH$ for 24 h and quenched the hot solution by pouring it into liquid nitrogen. After removal of all volatiles and drying of the residue, the polymer was redissolved in $CHCl_3/CF_3COOH$ (0.2 g/dL) to give the same $[\alpha]^{23}_D$ value (+3.0°) as that of the P(APP) before heat treatment (+3.1°, 0.2 g/dL), indicating no racemization took place under the current heat treatment conditions. We also synthesized P(APP) using (*S*,*S*)-**1** and obtained the P(APP) exhibiting opposite signs in both optical rotation and CD to those of the P(APP) by the enantiomeric (*R*,*R*) catalyst.

Polymerization of Methacrylates. Our above-described findings that optical activity was observed with the P(MMA)-*b*-P(acrylamide) block copolymers, even when the acrylamide homopolymers do not form a helical structure, led to a hypothesis that in synthesizing block copolymers with methacrylates, the mirror plane that exists in homopolymers that renders them cryptochiral could be eliminated, giving rise to optically active, nonhelical block copolymers. To ensure that the optical activity that could arise from the block copolymers was not influenced by chain-end groups, we systematically investigated the optical activity of enantiomeric P(MMA) to approximate the MW required to reach cryptochirality from polymers produced by our catalyst system (runs 32–35, Table 5). Similarly to the observations of Wulff,[7] the P(MMA) with $M_n = 2.56 \times 10^4$ g/mol ($P_n \approx 250$) shows minimal optical activity. A further increase in MW gives the polymer without any optical activity. Ensuring that the second block was also long enough to reach cryptochirality, we

polymerized *n*-butyl methacrylate (BMA) by (*S*,*S*)-**1** to find the M_n at which optical activity was not observed (run 36, Table 5).

In contrast to the optically active P(MMA)-*b*-P(acrylamide) block copolymers, the $P(MMA)_{400}$-*b*-$P(BMA)_{400}$ synthesized by (*S*,*S*)-**1** was, surprisingly, optically inactive (run 37, Table 5). To perturb the symmetry of the block copolymer further, we polymerized nonequivalent ratios of MMA and BMA by (*S*,*S*)-**1**, but still leading to an optically inactive copolymer (run 38, Table 5). Next, we produced random copolymer $P(MMA)_{400}$-*co*-$P(BMA)_{400}$, and it was found also optically inactive (run 39, Table 5). Lastly, we synthesized the ABC triblock methacrylate copolymer of MMA, BMA, and 2-ethylhexylmethacrylate (EHM) using (*S*,*S*)-**1**; again, the well-defined triblock copolymer ($M_w/M_n = 1.04$) showed no optical activity (run 40, Table 5). The sharp contrast between the optically active methacrylate-*b*-acrylamide block copolymers and methacrylate-*b*-methacrylate diblock or triblock copolymers may be explained by the following analysis: with the methacrylate-*b*-methacrylate block copolymers, the first nonequivalent atom from the asymmetric carbon on the main chain, in comparison of the two different monomer repeat units, is four atoms away, while the first nonequivalent atom between the two different monomers within the methacrylate-*b*-acrylamide block copolymers is attached directly to the asymmetric carbon.

Conclusions

We have investigated the kinetics and scope of the metallocene-mediated asymmetric coordination polymerization of acrylamide and methacrylate monomers using the enantiomeric catalysts (*S*,*S*)-**1** and (*R*,*R*)-**1** to produce optically active, stereoregular polymers of several different classes. Through kinetic studies it has been shown that the polymerization of *N*,*N*-diaryl acrylamides such as DPAA by **1** proceeds via a mechanism identical to the one already established for the polymerization of *N*,*N*-dialkyl acrylamides, namely a monometallic, coordination-conjugate addition process. In analyzing how chain length affects optical activity of polymers, we have shown that increasing MW will increase the optical activity of polymers which can form secondary structure of solution-stable helical conformations, whereas for random-coil polymers an increase in MW will gradually diminish the influence of chain-end groups on the overall chiroptical properties of the polymer, resulting in a decrease in optical activity to ultimately null when cryptochirality is reached.

The formation of optically active poly(acrylamide)s due to solution-stable helical conformations with an excess of one-handed helicity is dictated by the sterics and rigidity of the monomer repeat units. Diaryl acrylamides such as DPAA, PTAA, and HPPA are readily polymerized by the enantiomeric catalyst **1** to optically active helical polymers, with the unsymmetrically substituted monomers (PTAA and HPPA) giving the chiral polymers of much enhanced optical activity as compared to the one derived from symmetrically substituted DPPA. Introduction of the long-chain alkyl group to one the phenyl rings (i.e., HPPA) not only accomplishes the unsymmetrical substitution but also solves the solubility issue associated with rigid helical homopolymers, enabling direct MW analysis of such polymers by LS/GPC. All nondiaryl acrylamides investigated in this study led to nonhelical polymers, except for APP which was identified by MM2 modeling and successfully gave rise to the first optically active, helical poly(*N*,*N*-dialkyl acrylamide), P(APP).

We have also carried out extensive asymmetric block copolymerization studies of MMA with *N*,*N*-diaryl acrylamides to solve the solubility issue associated with helical homopolymers of acrylamides, to further confirm the living/controlled nature of the present polymerization system toward such polar monomers, and to produce the unique optically active, flexible random coil−rigid helical stereoblock copolymers. We further discovered that all the high-MW methacrylate-*b*-acrylamide block copolymers produced by the enantiomeric catalysts **1** are optically active, even when the MW of both blocks far exceeds their cryptochiral MW and regardless of whether the acrylamide comonomer employed can render solution-stable helical conformation or not. On the other hand, all the methacrylate-*b*-methacrylate well-defined stereodiblock or triblock copolymers produced by the enantiomeric catalysts **1** are optically inactive, which is attributable to the similar structures of the methacrylate repeat units placing the first nonequivalent atom between the different methacrylate units too far away from the asymmetric carbon center.

Acknowledgment. This work was supported by the National Science Foundation (NSF-0718061). We thank Prof. Alan Kennan (CSU) for assistance in CD measurements and Boulder Scientific Co. for the research gift of $B(C_6F_5)_3$.

References and Notes

(1) (a) For selected reviews, see Yashima, E.; Maeda, K. *Macromolecules* **2008**, *41*, 3–12. (b) Yamamoto, C.; Okamoto, Y. *Bull. Chem. Soc. Jpn.* **2004**, *77*, 227–257. (c) Nakano, T.; Okamoto, Y. *Chem. Rev.* **2001**, *101*, 4013–4038. (d) Cornelissen, J. J. L. M.; Rowan, A. E.; Nolte, R. J. M.; Sommerdijk, N. A. J. M. *Chem. Rev.* **2001**, *101*, 4029–4070. (e) Okamoto, Y.; Nakano, T. *Chem. Rev.* **1994**, *94*, 349–372. (f) Okamoto, Y.; Yashima, E. *Prog. Polym. Sci.* **1990**, *15*, 263–298. (g) Wulff, G. *Angew. Chem., Int. Ed. Engl.* **1989**, *28*, 21–37. (h) Pino, P. *Adv. Polym. Sci.* **1965**, *4*, 393–456.
(2) Farina, M. *Top. Stereochem.* **1987**, *17*, 1–111.
(3) Pino, P.; Cioni, P.; Wei, J. *J. Am. Chem. Soc.* **1987**, *109*, 6189–6191.
(4) Kaminsky, W.; Ahlers, A.; Möller-Lindenhof, N. *Angew. Chem., Int. Ed. Engl.* **1989**, *28*, 1216–1218.
(5) Pino, P.; Galimberti, M.; Prada, P.; Consiglio, G. *Makromol. Chem.* **1990**, *191*, 1677–1688.
(6) Kaminsky, W. *Angew. Makromol. Chem.* **1986**, *145/146*, 149–160.
(7) Wulff, G.; Zweering, U. *Chem. Eur. J.* **1999**, *5*, 1898–1904.
(8) Beckerle, K.; Manivannan, R.; Lian, B.; Meppelder, G.-J. M.; Raabe, G.; Spaniol, T. P.; Ebeling, H.; Pelascini, F.; Mülhaupt, R.; Okuda, J. *Angew. Chem., Int. Ed.* **2007**, *46*, 4790–4793.
(9) Wulff, G.; Dhal, P. K. *Angew. Chem., Int. Ed. Engl.* **1989**, *28*, 196–198.
(10) Wulff, G. *Polym. News* **1991**, *16*, 167–173.
(11) (a) Coates, G. W.; Waymouth, R. M. *J. Am. Chem. Soc.* **1993**, *115*, 91–98. (b) Coates, G. W.; Waymouth, R. M. *J. Am. Chem. Soc.* **1991**, *113*, 6270–6271.
(12) Yeori, A.; Goldberg, I.; Kol, M. *Macromolecules* **2007**, *40*, 8521–8523.
(13) (a) Nakano, T.; Okamoto, Y. Hatada, K. *J. Am. Chem. Soc.* **1992**, *114*, 1318–1329. (b) Okamoto, Y.; Suzuki, K.; Ohta, K.; Hatada, K. Yuki, H. *J. Am. Chem. Soc.* **1979**, *101*, 4763–4765.
(14) (a) Shiohara, K.; Habaue, S.; Okamoto, Y. *Polym. J.* **1998**, *30*, 249–255. (b) Okamoto, Y.; Hayashida, H.; Hatada, K. *Polym. J.* **1989**, *21*, 543–549. (c) Okamoto, Y.; Adachi, M.; Shohi, H.; Yuki, H. *Polym. J.* **1981**, *13*, 175–177.
(15) (a) For selected recent examples of helix-sense-selective polymerization, see Tang, H.-Z.; Garland, E. R.; Novak, B. M.; He, J.; Polavarapu, P. L.; Sun, F. C.; Sheiko, S. S. *Macromolecules* **2007**, *40*, 3575–3580. (b) Tsuji, M.; Azam, A. K. M. F.; Kamigaito, M.; Okamoto, Y. *Macromolecules* **2007**, *40*, 3518–3520. (c) Kajitani, T.; Okoshi, K.; Sakurai, S.-I.; Kumaki, J.; Yashima, E. *J. Am. Chem. Soc.* **2006**, *128*, 708–709. (d) Tang, H.-Z.; Boyle, P. D.; Novak, B. M. *J. Am. Chem. Soc.* **2005**, *127*, 2136–2142. (e) Tian, G.; Lu, Y.; Novak, B. M. *J. Am. Chem. Soc.* **2004**, *126*, 4082–4083. (f) Aoki, T.; Kaneko, T.; Maruyama, N.; Sumi, A.; Takahashi, M.; Sato, T.; Teraguchi, M. *J. Am. Chem. Soc.* **2003**, *125*, 6346–6347.
(16) (a) Azam, A. K. M. F.; Kamigaito, M.; Okamoto, Y. *J. Polym. Sci., Part A: Polym. Chem.* **2007**, *45*, 1304–1315. (b) Hoshikawa, N.; Hotta, Y.; Okamoto, Y. *J. Am. Chem. Soc.* **2003**, *125*, 12380–12381. (c) Nakano, T.; Okamoto, Y. *Macromolecules* **1999**, *32*, 2391–2393. (d) Nanano, T.; Shikisai, Y.; Okamoto, Y. *Polym. J.* **1996**, *28*, 51–60.
(17) (a) Serizawa, T.; Hamada, K.-I.; Akashi, M. *Nature* **2004**, *429*, 52–55. (b) Serizawa, T.; Hamada, K.; Kitayama, T.; Fujimoto, N.; Hatada, K.; Akashi, M. *J. Am. Chem. Soc.* **2000**, *122*, 1891–1899. (c) Hatada, K.; Kitayama, T.; Ute, K.; Nishiura, T. *Macromol. Symp.* **1998**, *132*,

221–230. (d) Spevacek, J.; Schneider, B. *Adv. Colloid Interface Sci.* **1987**, *27*, 81–150.
(18) Wulff, G.; Petzoldt, J. *Angew. Chem., Int. Ed. Engl.* **1991**, *30*, 849–850.
(19) Bolig, A. D.; Chen, E. Y.-X. *J. Am. Chem. Soc.* **2004**, *126*, 4897–4906.
(20) Rodriguez-Delgado, A.; Chen, E. Y.-X. *Macromolecules* **2005**, *38*, 2587–2594.
(21) (a) Mariott, W. R.; Chen, E. Y.-X. *Macromolecules* **2005**, *38*, 6822–6832. (b) Mariott, W. R.; Chen, E. Y.-X. *Macromolecule* **2004**, *37*, 4741–4743.
(22) Miyake, G. M.; Mariott, W. R; Chen, E. Y.-X. *J. Am. Chem. Soc.* **2007**, *129*, 6724–6725.
(23) Allen, R. D.; Long, T. E.; McGrath, J. E. *Polym. Bull.* **1986**, *15*, 127–134.
(24) Kim, Y. C.; Jeon, M.; Kim, S. Y. *Macromol. Rapid Commun.* **2005**, *26*, 1499–1503.
(25) Kim, Y.-J.; Bernstein, M. P.; Galiano Roth, A. S.; Romesber, F. E.; Williard, P. G.; Fuller, D. J.; Harrison, A. T.; Collum, D. B. *J. Org. Chem.* **1991**, *56*, 4435–4439.
(26) (a) Grossman, R. B.; Doyle, R. A.; Buchwald, S. L. *Organometallics* **1991**, *10*, 1501–1505. (b) Collins, S.; Kuntz, B. A.; Taylor, N. J.; Ward, D. G. J. *Organomet. Chem.* **1988**, *342*, 21–29.
(27) Diamond, G. M.; Jordan, R. F.; Petersen, J. L. *J. Am. Chem. Soc.* **1996**, *118*, 8024–8033.
(28) LoCoco, M. D.; Jordan, R. F. *J. Am. Chem. Soc.* **2004**, *126*, 13918–13919.
(29) Rodewald, S.; Jordan, R. F. *J. Am. Chem. Soc.* **1994**, *116*, 4491–4492.
(30) Mariott, W. R.; Rodriguez-Delgado, A.; Chen, E. Y.-X. *Macromolecules* **2006**, *39*, 1318–1327.

MA8000675